UNIVERSITAT POLITÈCNICA DE VALÈNCIA

DEPARTAMENT DE MATEMÀTICA APLICADA

UNIVERSITAT POLITÈCNICA DE VALÈNCIA

Dpto. de Matemática Aplicada

Modelización de la difusión de la bacteria Candida Auris en el entorno de una Unidad de Cuidados Intensivos (UCI)

Trabajo Fin de Máster

Máster Universitario en Investigación Matemática

AUTOR/A: Perez Diukina, Cristina

Tutor/a: Villanueva Micó, Rafael Jacinto

Cotutor/a: Cortés López, Juan Carlos

CURSO ACADÉMICO: 2021/2022

A mathematical model of Candida Auris in the ICU

Author: Cristina Pérez-Diukina

Supervisors: Dr Juan Carlos Cortés López

Dr Rafael-Jacinto Villanueva Micó

UNIVERSITAT POLITÈCNICA DE VALÈNCIA

DEPARTAMENT DE MATEMÀTICA APLICADA

Abstract

The multi-drug resistant yeast Candida Auris (CA) poses a global threat to the healthcare environment. In this work, we have applied the Fisher Kolmogorov-Petrovsky–Piskunov (FKPP) equation to model the change in density trough time of CA. inside an Intensive Care Unit (ICU). Such a model will allow us to evaluate the efficacy of well timed cleaning measures on CA. population control at the ICU.

Contents

Introduction

The importance of Mathematical Modeling in Biology and Medicine

If constructed with the collaboration of both mathematicians and medical personnel, mathematical models can provide valuable support to experts in the fields of biology and medicine. When supported by computer aided simulations they can help us to better understand complex biological systems and make reliable predictions.

In order to model a population of microorganisms in a given environment through time and space, ordinary differential equations (ODEs) and partial differential equations (PDEs) are, respectively, well studied and valuable tools. In practice, exact solutions are few and numerical solutions are often used to describe the dynamic behaviour of the population through time. In order to assert that the numerical solutions are modelling real world phenomena it is important to calibrate these models with biological and physical data.

Contents

In this work we present a mathematical model to describe the diffusion of a yeast, CA, within an ICU.

In Chapter 1 we introduce CA's characteristics and the problem it represents for a healthcare environment such as an ICU. Then, in the Chapter 2 we jump into the mathematical model itself. After that, in the Chapter 3 we explain how the parameter calibration was performed to fit this model to real world data. Lastly, in the Chapter 4, we show the results of simulations performed with Matlab.

Chapter 1

Candida Auris, a short overview

Candida Auris (CA) is a multi-drug resistant yeast that poses a threat to the global health system, and in particular, to the vulnerable Intensive Care Unit (ICU) patients. In this chapter we give a quick overview on CA's characteristics and why it is a threat in the ICU environment.

1.1 A short summary of CA's characteristics

Candida Auris (CA) is a multi-drug resistant yeast that was found in 2009 in the ears of a Japanese and South Korean patients [23, 7]. It has quickly spread around the world and has now been identified in more than 30 countries. Four major clades have been distinguished in Africa, South America, East Asia, and South Asia [6].

CA is able to colonise different body parts, like skin or mucous membranes, with an optimal growth temperature of $37-40^oC$ (around normal human body temperatures and temperatures of those suffering from a fever), and it still grows at temperatures of up to 45^oC (for temperatures higher or equal to 45^oC its population decays) [23].

CA has been observed to express several virulence factors such as the formation of microorganism communities called biofilms [14]. Microorganisms within a biofilm have been found to be much more resistant to drugs, in part due to the ability of biofilm cells to tolerate some antibiotics such as ampicillin [21].

Some strains of CA also display Antimicrobial Resistance (AMR). AMR is the ability of a microorganism (virus, bacteria, parasite or fungus) to survive and grow in the presence of antimicrobial drugs.

1.2 A global threat

This relatively new species of yeast is a public health concern in the healthcare settings and particularly in the ICU environment across the globe [22].

CA can cause superficial candidiasis and also invasive infections such as intra-abdominal candidiasis, chronic otitis media, and bloodstream infections. These complications are more likely to occur in severely ill and immunosuppressed patients admitted to ICU. This yeast is primarily transmitted from a colonized (meaning that they carry the pathogen but are not infected themselves) or infected patient to uncontaminated healthcare workers. A colonized or infected patient can also excrete this pathogen into their environment. Therefore, the main reservoir of CA pathogens is the contaminated hands of healthcare workers and their environment, including reusable parts of observation and diagnostic equipment, which play a major role in the onward transmission of infections among ICU patients [8, 10, 24].

As far as we know, the information available about CA is rather limited and heterogeneous, particularly regarding the mortality rates. The mortality rates associated with CA vary greatly from study to study depending on the country and the environment in which infected subjects were located, but overall is high, with a crude

mortality ranging from 30% to 72% [17]. The crude mortality rate is defined by the Centers for Disease Control and Prevention (CDC) as the "total number of deaths during a given time interval" [20].

AMR of some strains of CA not only impedes population control of this microorganism in healthcare settings, but also poses a serious threat to the global population. Although in recent years the World Health Organization (WHO), the United Nations General Assembly and other organizations have declared AMR as one of the top ten global public health threats to humanity [2]. Inaction in the face of this problem has continued for the past fifty years. In numerous high-impact scientific studies, researchers acknowledge the important advances in public health thanks to antibiotic treatments, but warn about the uncontrolled prescription of antibiotic drugs and the overuse of antibiotics in the food industry [27, 18].

Environmental CA sample have shown presence of CA on many horizontal surfaces such as floors and keyboards. Furthermore, CA is also able to survive on plastic surfaces, wich readily present in ICUs, for at least 2 weeks [26]. These microbiological characteristics are partly due to CA's ability to form biofilms, making it resistant to multiple cleaning agents commonly used in healthcare settings [22].

Because the ICU population is particularly vulnerable, these attributes pose a significant threat. After the colonization of an ICU patient with CA, if no prevention measures were to be taken, it is estimated that the whole ICU would be colonized within 48h [1]. Therefore, ICU personnel have to undertake costly measures to control the spread of CA such as weekly testing of patients, isolation of detected colonized patients, and in depth cleaning.

To face this problem, mathematical models allow us to simulate the CA population spread in a environment such as ICU in a time and cost efficient manner.

[1] information provided by chief ICU medical personnel (Hospital General de Castellón).

Because the number of people inside an ICU is limited and rather small we concluded that SIR models (which model much bigger populations) do not seem to be the best choice. Recently, the study of the dynamics of microorganism populations in biofilms has shown that the diffusion of these micro-populations resembles the expansion of urban communities [19]. Schematically, an outbreak could be represented as a bell shaped function that spreads through its environment like a wave . Hence, the models for 2D heat waves appears to be adequate for modelling the level of contamination of an ICU room at a given time.

In this work, we propose to model the biological diffusion of CA within the ICU using with the Fisher Kolmogorov–Petrovsky–Piskunov (FKPP) model [25]. To calibrate the model's parameters, CA *in vitro* growth data and expert ICU medical personnel information have been used.

Chapter 2

Model Overview

In this chapter we introduce the Fisher Kolmogorov–Petrovsky–Piskunov reaction-diffusion equation. We shortly discuss the existence of a unique solution of this system and then introduce a cleaning factor into our model.

2.1 Fisher Kolmogorov–Petrovsky–Piskunov Equation

The 2-dimensional Fisher Kolmogorov–Petrovsky–Piskunov (Fisher–KPP) model is a reaction-diffusion system that is used to model population growth in a two dimensional coordinate space through time [25], given by the following equation:

$$\frac{\partial u}{\partial t} = D\left(\frac{\partial^2 u}{\partial x^2} + \frac{\partial^2 u}{\partial y^2}\right) + ru(1-u), \tag{2.1}$$

where x and y are the coordinates of a point on a plane, u is the density of the population in $[a,b] \times [c,d]$, $a,b,c,d \in \mathbb{R}$ at a given time t, $D > 0$ is the diffusion coefficient and $0 \leq r \leq 1$ is the growth rate.

In this model the variation of the population density u through time is guided by both the diffusion term $D\left(\frac{\partial^2 u}{\partial x^2} + \frac{\partial^2 u}{\partial y^2}\right)$ which models microorganism's expansion in a plane, and the population growth term $ru(1-u)$, which indicates the amount of CA at a given time, with restricted growth, as it is assumed that the environment has a limited amount of resources.

Theorem 2.1.1. *Given arbitrary initial conditions at time $t = 0$ satisfying*

$$0 \leq u \leq 1. \tag{2.2}$$

The PDE

$$\frac{\partial u}{\partial t} = D\frac{\partial^2 u}{\partial x^2} + f(u)$$

has one and only one solution for $t > 0$ satisfying (2.2) [2] if it is true that

1. $f(0) = f(1) = 0$,
2. $f(u) > 0,\ 0 < u < 1$,
3. $f'(0) = 1$,
4. $f'(u) < 1,\ 0 < u \leq 1$,
5. $f'(u)$ *is bounded and continuous on* $(0, 1)$,
6. $f(u)$ *is sufficiently differentiable.*

It is easy to see that, if $r = 1$, $f(u) = ru(1-u)$ satisfies conditions $(1) - (6)$ since $f'(u) = 1 - 2u$ and $f(u) \in C^\infty$ (set of all infinitely differentiable functions).

[2] The proof by Andrey Nikolaevich Kolmogorov can be found in *"Selected Works of AN Kolmogorov: Volume I: Mathematics and Mechanics"* pages $255 - 270$ [25].

In general, and for higher dimensions, it has been proven that there exists a unique weak solution

Theorem 2.1.2. *Suppose that*

$$\frac{\partial u}{\partial t} = D\left(\frac{\partial^2 u}{\partial x^2} + \frac{\partial^2 u}{\partial y^2}\right) + f(u) \tag{2.3}$$

is defined on $U \times (0, T]$ *where* $U \subset \mathbb{R}^n$*, open and bounded with smooth boundary* ($\partial U \in C^1$) *and* $T > 0$ *is fixed. If* $u(x, y, t) = 0$ *on the boundary of* U *for all* $t \in (0, T]$*,* $u(x, y, 0) = g(x, y)$ *where* $g \in H_0^1(U; \mathbb{R}^m)$*, a subset of a Sobolev space* (H^1)*, and* f *is Lipschitz continuous, then there exists a unique weak solution of* (2.3). [3]

Now we can apply this result to (2.1), since $f(u) = u(1 - u),\ u \in [0, 1]$ which is Lipschitz continuous since $u' = r(1 - 2u) \leq 1$ since $r \in (0, 1)$ and $u \in [0, 1]$. Thus taking an initial condition $u(x, y, 0) = g(x, y)$, where $g \in H_0^1(U; \mathbb{R}^m)$ will ensure a unique weak solution to this PDE.

However, the closed solution to the FKPP equation is not known. We thus have to solve it numerically, which we will discuss in more detail in Chapter 4.

2.2 Introduction of a cleaning factor

The ICU is cleaned regularly by trained staff in order to minimize the spread of any harmful microorganism. To model this we introduce a cleaning factor into our model. We assume that the ICU is cleaned in a uniform manner. So at times separated by equal intervals, the amount of CA is reduced by some percent at every

[3] Proof using Banach's fixed point theorem available in [9] Chapter 9.2.

point (x, y) on the plane. Then when this is introduced to the model, the amount of CA in the ICU at every point (x, y) on the plane and time t is

$$u(x, y, t) = \begin{cases} p\hat{u}(x, y, t), \text{ if cleaning happend at time } t, \\ \hat{u}(x, y, t), \text{ otherwise.} \end{cases} \tag{2.4}$$

where $\hat{u}(x, y, t)$ is the numeric solution to equation (2.1) and $p \in (0, 1)$ represents the efficacy of the cleaning product used. We will explore two cases, when p is the same for all the points, or when p follows a given density distribution function.

Chapter 3

Model Parameter Estimation

In this chapter we solve the FKPP equation numerically in Matlab. We then calibrate our model so that it matches real-life data of CA in-vitro growth.

We begin our parameter estimation by solving and fitting the logistic growth part of the FKPP system without worrying about the diffusion term for now. Since it has a nonlinear closed form solution we will use Nonlinear Least Squares to do so.

3.1 Nonlinear Least Squares

We will first give a short overview of the least squares estimation method for nonlinear functions where the parameters are unknown. For further detail on nonlinear methods, consult [5].

Suppose our observed data is (x_i, y_i) $, i = 1, \ldots, n$ and we know f, its functional relationship if no noise were to be present in the observed data. Taking the noise into consideration, we have:

$$y_i = f(x_i, \theta_T) + \epsilon_i,\ i = 1, \ldots, n \tag{3.1}$$

with $E(\epsilon_i) = 0,\ \theta_T \in \Theta \subset \mathbb{R}^p$ (here $E(\cdot)$ denotes the expectation operator) where θ_T is a vector with parameters of f to be estimated.

We denote the least squares estimate of θ_T as $\hat{\theta}$. $\hat{\theta}$ is such that it minimizes the sum of squares:

$$S(\theta) = \sum_{i=1}^{n} [y_i - f(x_i, \theta)]^2$$

over $\theta \in \Theta$.

We also assume that $\epsilon_i \sim M(0, \sigma^2)$, *iid* (independently and identically distributed) where the continuous probability distribution M is not known. Further, $\hat{\epsilon} = [y_i - f(x_i, \hat{\theta})]_{i=1,\ldots,n}$

If we assume that M is a normal distribution, then $\hat{\theta}$ is also the maximum-likelihood estimator.

If it is true that every $f(x_i, \theta),\ i = 1, \ldots, n$ is differentiable with respect to θ and $\hat{\theta} \in int(\Theta)$, then

$$\left.\frac{\partial S(\theta)}{\partial \theta_r}\right|_{\hat{\theta}} = 0. \tag{3.2}$$

Let $f_i(\theta) \coloneqq f(x_i, \theta)$, and $\boldsymbol{f}(\theta) = (f_1(\theta), \ldots, f_n(\theta))'$. Then we denote $\boldsymbol{F}(\theta) \coloneqq \frac{\partial f(\theta)}{\partial \theta}$. We also denote $\hat{\boldsymbol{F}} \coloneqq \boldsymbol{F}(\hat{\theta})$.

Then by (3.2), we can write

$$\sum_{i=1}^{n}[y_i - f_i(\theta)] \times \frac{\partial S(\theta)}{\partial \theta_r}\bigg|_{\hat{\theta}} = 0,\ i = 1, \ldots, p,$$

which can be rewritten as

$$0 = \hat{\boldsymbol{F}} \times \hat{\epsilon}. \tag{3.3}$$

The equation (3.3) is called the normal equation and for most non-lineal models it cannot be solved analytically [5]. We thus choose to solve it numerically using the R package *nls* [4].

We first solve the logistic growth equation $\frac{\partial u}{\partial t} = ru(1-u)$.

The closed-form solution is

$$u(t) = \frac{u_0 \exp(rt)}{u_0(\exp(rt) - 1) + 1}, \tag{3.4}$$

where u_0 is the initial normalized quantity of CA in the ICU. So here f is (3.4), and $\theta = (r, u_0)$.

In order to estimate the growth rate, r, and the initial value, u_0, the solution to the logistic growth model (3.4) has been fitted to CA *in vitro* growth data [11] using nonlinear least squares (Figure 3.1).

The *in vitro* growth data comes from experimental strains of CA inoculated onto Sarcocystis dextrose agar. These strains were incubated for 24 hours at a constant temperature of 37^oC.

We have found the approximate growth rate to be $\hat{r} = 0.30955$ and $\hat{u}_0 = 0.01507$, with a residual sum-of-squares of 0.1353. These two results give us an estimate of the parameter space in which to calibrate the model and a way to choose an initial condition that fits the data.

3.2 Numerical solution of the FKPP

We choose to solve the FKPP model numerically using Matlab. We use explicit finite differences. We decide to set Neumann, no flux boundary conditions. We set a spatial integration step h and a temporal step k and we discretize the FKPP equation by evaluating it at the points $(x_i, y_l, t_j),\ i = 1, 2, \ldots, nx,\ l = 1, 2, \ldots, ny,\ j = 1, 2, \ldots, T$. We further suppose that $N \coloneqq nx = ny$ making our ICU plane a square. We are aware that this is a simplification but it is a first approach to the problem.

We take as an approximation of the temporal derivative the foward difference

$$\frac{\partial u(x,y,t)}{\partial t} \approx \frac{u(x,y,t+k) - u(x,y,t)}{k} = \frac{u_{i,l,j+1} - u_{i,l,j}}{k}$$

and for the spatial derivative we take the centered differences, giving us

$$\begin{aligned}\frac{\partial^2 u(x,y,t)}{\partial x^2} &\approx \frac{u(x+h,y,t) - 2u(x,y,t) + u(x-h,y,t)}{h^2} \\ &= \frac{u_{i+1,l,j} - 2u_{i,l,j} + u_{i-1,l,j}}{h^2},\end{aligned}$$

$$\begin{aligned}\frac{\partial^2 u(x,y,t)}{\partial y^2} &\approx \frac{u(x,y+h,t) - 2u(x,y,t) + u(x,y+h,t)}{h^2} \\ &= \frac{u_{i,l+1,j} - 2u_{i,l,j} + u_{i,l-1,j}}{h^2}.\end{aligned}$$

Putting all of these together and solving for the largest time step we get

$$u_{i,l,j+1} = \frac{kD}{h^2}\big(u_{i+1,l,j} + u_{i,l+1,j} - 4u_{i,l,j} + u_{i-1,l,j} + u_{i,l-1,j}\big) + u_{i,l,j} + kru_{i+1,l,j}(1 - u_{i+1,l,j}),$$

which we can rewrite in matrix form as follows

$$u^{(j+1)} = \frac{kD}{h^2}Au^{(j)} + u^{(j)} + kru^{(j)} \circ (1 - u^{(j)})$$

$$\mathrm{u}^{(j)} = \begin{bmatrix} u_{1,1,j} = 0 \\ u_{2,1,j} \\ u_{3,1,j} \\ \vdots \\ u_{N,1,j} = 0 \\ \vdots \\ u_{1,N,j} = 0 \\ \vdots \\ u_{N,N,j} = 0 \end{bmatrix} \tag{3.5}$$

for $j = 1, \ldots, T$, where A is a $N^2 \times N^2$ matrix with all zeroes except at the main diagonal, D_0, off 1 diagonals, D_{-1}, D_1 and off 10 diagonals,D_{-N}, D_N. Here $\circ$ denotes the Hadamard product.

$$D_0 = \big(\overbrace{0 \ \ldots \ 0}^{N+1} \quad \overbrace{-4 \ \ldots \ -4}^{N^2-2N+2} \quad \overbrace{0 \ \ldots \ 0}^{N+1}\big)$$

$$D_1 = D_{-1} = \big(\overbrace{0 \ \ldots \ 0}^{N} \quad \overbrace{1 \ \ldots \ 1}^{N^2-2N-1} \quad \overbrace{0 \ \ldots \ 0}^{N}\big)$$

$$D_{-N} = \big(0 \quad \overbrace{1 \ \ldots \ 1}^{N-2} \quad 0 \ \ 0 \quad \overbrace{1 \ \ldots \ 1}^{N-2} \quad \ldots\big)$$

$$D_N = \big(\overbrace{0\ \dots\ 0}^{N+1}\quad \overbrace{1\ \dots\ 1}^{N-2}\quad 0\ \ 0\quad \overbrace{1\ \dots\ 1}^{N-2}\quad \dots\big)$$

This numerical solution has error $O(h + k^2)$.

We built a 101×101 mesh-grid to model the plane representing the ICU where $x \in \{0, 0.1, 0.2, \dots, 10\}$ and $y \in \{0, 0.1, 0.2, \dots, 10\}$, which sets the spatial step to be $h = 0.1$. The FKPP equation is parabolic

We let the time go from 0 to 48 with a time step of

$$k = \min\{0.5, 0.99\frac{h^2}{4D}\}$$

so that $k < \frac{h^2}{4D}$ in order to guarantee stability in the numerical scheme [16, 15], but we can also achieve higher resolutions if $\frac{h^2}{4D}$ is small enough.

To numerically solve the F-KPP model, we need to define our initial condition, which we want to both agree with previous results and literature on microorganism populations.

The dynamics of microorganism populations in biofilms have been shown to share structural aspects with urbanizations [19]. We assume that the outbreak of CA is a city (set of densely populated microcolonies enclosed to well-defined boundaries) as defined by Paula Amauri, Geelsu Hwang, and Hyun Koo and resembles schematically a dome [19]. Therefore, we want our initial condition (IC) of to be bell shaped and represents the accumulation of CA cells. For simplicity, we will set the IC as to model an outbreak located in the center of the ICU. In order for the IC to agree with previous results of nonlinear least squares, where $u_0 = 0.01507 \approx 10^{-2}$ (Section 3.1), we also want to set the initial amount of CA in the ICU,

$$\int_0^{10}\int_0^{10} u(x,y,0)dxdy,$$

estimated here as the sum of $u(x,y,t)$ over all the points of the mesh-grid at times 0, to be around 10^{-2} on the normalized scale of 0 to 1. We recall that $u \in [0,1]$, meaning that the maximum density of CA at any point (x,y) is 1. The orange points in Figure 3.1 , that represent real growth data, reach 1 after 24 hours, and because we chose the logistic growth, it will plateau there and remain at the last time instance 48. So we know that in our model the maximum will be achieved when the mesh-grid has values of 1 everywhere except in the four corners (that are always 0). Since we have built a 101×101 mesh-grid, we will get $10201 - 4 = 10197$ points evaluated at 1. In our discretization, our estimate of $\int_0^{10}\int_0^{10} u(x,y,48)dxdy$ is $0.1^2 \sum\sum_{x,y\in\{0,0.1,0.2,\ldots,10\}} u(x,y,48)$ so the maximum sum will be $1.0197 \times 10^4 \times 10^{-2} = 101.9700$, which is our normalizing constant.

We set the initial condition of the problem to be

$$u(x,y,0) = \exp\{3\big(-(x-5)^2-(y-5)^2\big)\}. \tag{3.6}$$

This function is bell shaped and centered in the middle of our $[0,10]^2$ ICU plane and

$$\int_0^{10}\int_0^{10} \exp\{3\big(-(x-5)^2-(y-5)^2\big)\big)dxdy \approx 1.05$$

giving us, after normalization $1.05/101.9700 \approx 0.0103$ which is around 1×10^{-2} as wanted. Therefore the function in equation (3.6) seems to be an appropriate initial condition.

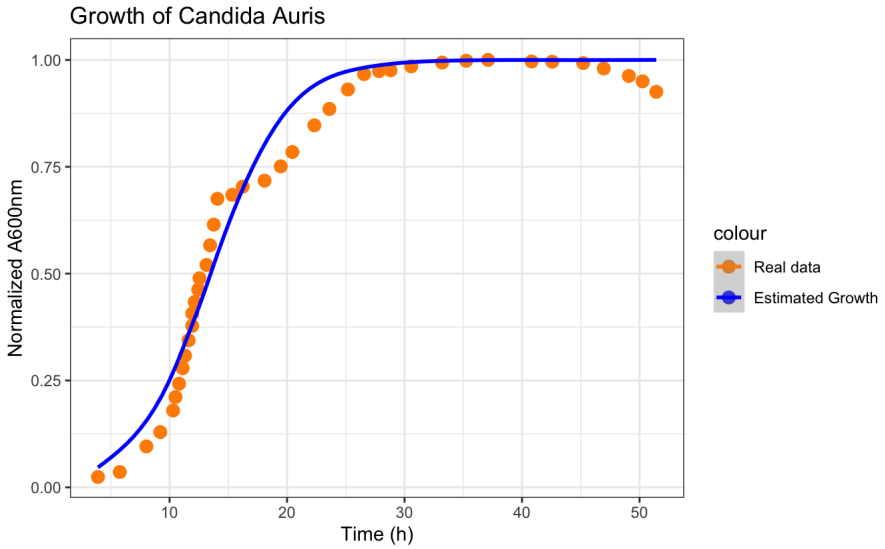

Figure 3.1: Observed *in vitro* growth of CA and estimated logistic growth using nonlinear least squares.

In our numerical solution we set Neumann boundary conditions, where the four corners of the ICU plane have no flux and are maintained to be 0.

3.3 Particle Swarm Optimization

We then applied Particle Swarm Optimization (PSO) to calibrate both the diffusion coefficient D and the growth coefficient r simultaneously. PSO is a numeric biologically derived search algorithm, fist introduced by Kennedy and Eberhar in 1995 [12]. When searching for optimal parameters that minimize a given function, it searchers the parameter space. It is a computationally very effective algorithm. The data we mentioned in the previous part (plotted in Figure 3.1) shows that the normalized $A600nm$ (absorbance at $600nm$ wavelength) readings of CA reaches 1 at about 20h and is more or less mantained at 1 for the next 30 or so hours.

Let $f(t) = \int_0^{10} \int_0^{10} u(x, y, t)dxdy$ and $\{z_1, ..., z_n\}$ be the observed CA growth data.

We define as the objective function for the PSO to minimize, the Symmetric Mean Absolute Percentage Error (SMAPE)

$$S = \frac{1}{n}\sum_{i=1}^{n}\frac{|z_i - f(t_i)|}{\frac{|z_i|-|f(t_i)|}{2}} \tag{3.7}$$

where $\{t_1, t_2, \ldots, t_n\}$ is the set of times where CA's $A600nm$ (absorbance at $600nm$ wavelength) was measured.

We replace $f(t_i)$ with

$$\hat{f}(t_i) = 0.1^2 \sum_{x,y\in\{0,0.1,0.2,\ldots,10\}}\sum u(x, y, t_i)$$

for all $i \in \{1, \ldots, n\}$ to get the discritized estimate of S

$$\hat{S} = \frac{1}{n}\sum_{i=1}^{n}\frac{|z_i - \hat{f}(t_i)|}{\frac{|z_i|+|\hat{f}(t_i)|}{2}} \tag{3.8}$$

Using the results from the initial parameter estimation, we search for (D, r) in $[0.0001, 1]^2$. The *particleswarm* function in Matlab allows us to calibrate the model using PSO with ease. This function has many parameters which one can tune. We chose to modify the default parameters for *SwarmSize*, which is the number of particles in the swarm (and is by default $\min\{100, 10 * \text{number of variables to estimate}\}$), and *MaxIterations*, which is the maximum number of iterations (which is by default $200 * (\text{number of variables to estimate})$).

The parameters $\hat{D} = 0.4141,\ \hat{r} = 0.3539$ were obtained after 68 iterations when the relative change in the objective value was less than $1e{-}6$. The objective function $\hat{S}$ was evaluated at 0.1160. Figure 3.2 shows that the estimated growth follows the observed data closely, except between 15 and 25 hours and after 43 hours, where there are sudden drops in the observed data that could not be captured by the logistic growth. Figure 3.3 illustrates the diffusion of CA throughout the ICU room, with CA being present everywhere in the room after 25 hours and being completely contaminated at 48 $hours$ (meaning that the density of CA is 1 everywhere).

When we first set the objective function to be the Mean Squared Error, we obtained $\hat{D} = 0.9803, \hat{r} = 0.3423$ (described in more detail in the Appendix in section 4.2.2). The results for SMAPE shows a decrease in D, which could be more realistic approximation of the diffusion term in the ICU environment since the temperature there is maintained at 23^oC instead of the 37^oC from the data (which is closer to CA's optimal growth temperature). Hence, for the rest of this work we use $\hat{D} = 0.4141,\ \hat{r} = 0.3539$ as our fixed parameters.

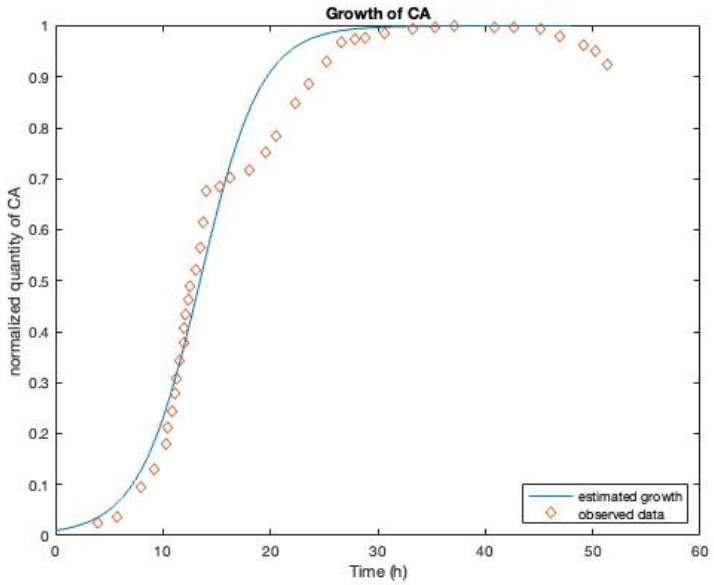

Figure 3.2: Observed *in vitro* growth of CA (points in orange) and $\hat{f}(t_i)$) (blue line) estimated using PSO and SMAPE error.

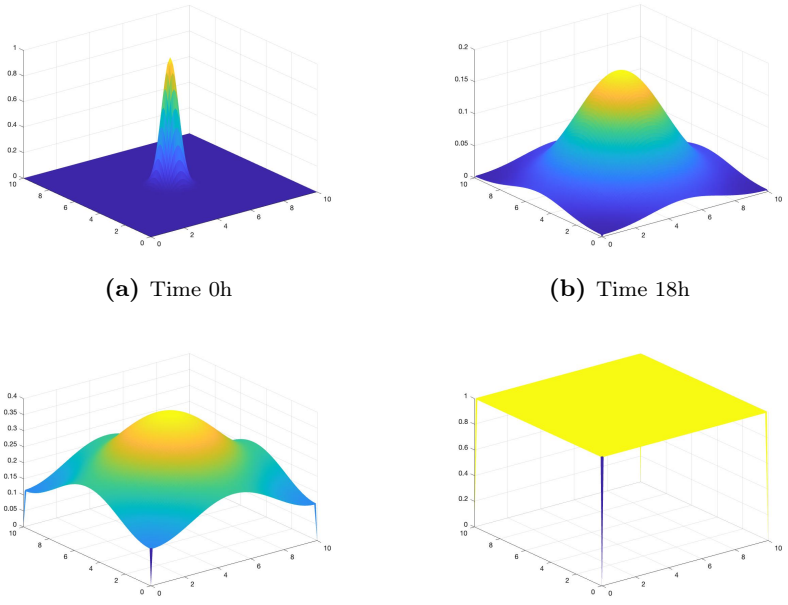

(a) Time 0h

(b) Time 18h

(c) Time 25h

(d) Time 48h

Figure 3.3: 3D plots of the FKPP numeric solutions when $\hat{r} = 0.3539,\ \hat{D} = 0.4141$

Chapter 4

Simulations

In this chapter we proceed to run several simulations using Matlab. We first vary the location of the outbreak, and the number of outbreaks present in the room by changing the initial condition in our model. We then introduce a cleaning factor that reduces the amount of CA in a timed a homogeneous manner.

4.1 Simulations of different initial conditions

Now that we have calibrated the model, using $\hat{D}$ and $\hat{r}$ we run several simulations to observe the changes in the systems behavior. While maintaining the optimal parameters estimated in Chapter 3 we change the initial condition in several ways.

First we change the location of the outbreak of CA in the ICU plane.

The contour plot 4.1 of the initial condition defined in equation (3.6) shows that the bell representing a concentration of CA cells has a radius of 1. We will re-center the function in order to start define different locations and number of outbreaks on the

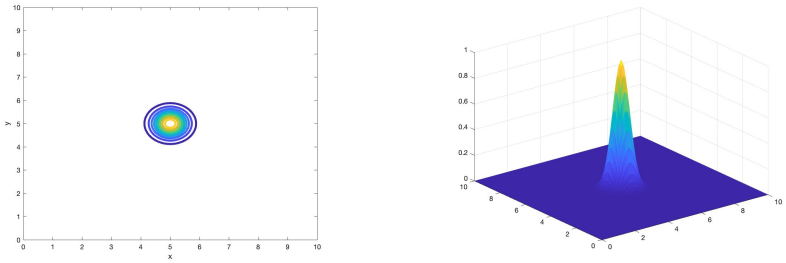

(a) 2D contour plot **(b)** 3D plot

Figure 4.1: 3D plot and 2D plot of $u(x, y, 0)$ with Initial Condition 1 (IC 1)

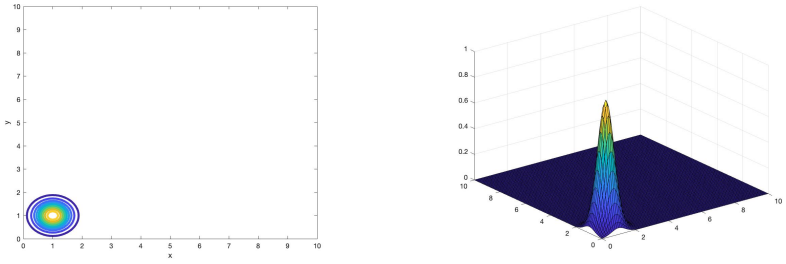

(a) 2D contour plot **(b)** 3D plot

Figure 4.2: 3D plot and 2D plot of $u(x, y, 0)$ with Initial Condition 2 (IC 2)

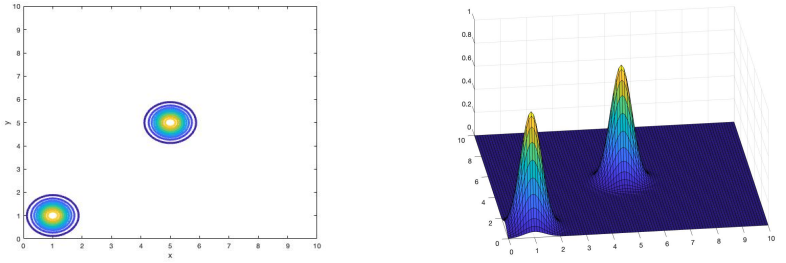

(a) 2D contour plot **(b)** 3D plot

Figure 4.3: 3D plot and 2D plot of $u(x, y, 0)$ with Initial Condition 3 (IC 3)

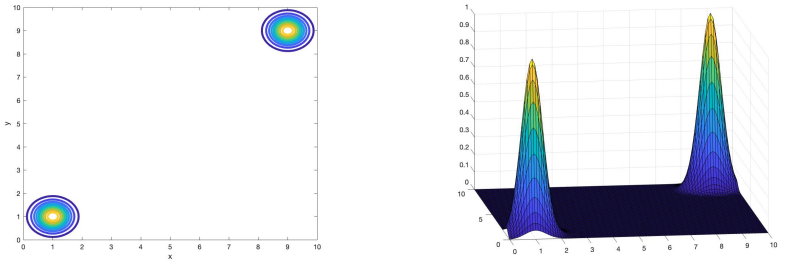

(a) 2D contour plot **(b)** 3D plot

Figure 4.4: 3D plot and 2D plot of $u(x, y, 0)$ with Initial Condition 4 (IC 4)

ICU plane. We recall that when calibrating the model $u(x, y, 0)$ was centered in the middle of the ICU.

We define three new initial conditions:

IC2 One outbreak located in one of the four corners of the ICU, shown in Figure4.2.

IC3 Two outbreaks: one located in the center, the second located in the corner, shown in Figure4.3.

IC4 Two outbreaks: located in opposite corners, shown in Figure4.4.

We then run our algorithm in Matlab as was done in Chapter 4 and just change the initial condition. Figure 4.8 compares the values on $\hat{f}$ for all four initial conditions. As expected, and shown in Figure 4.5 IC 2 has the slowest growth of all four initial conditions, as the outbreak starts in the corner and it takes longer for the wave to fill the ICU room.

The third case, IC 3, has outbreaks located relatively close and through our simulation we can observe that the centered wave merges into the corner wave. It is interesting to note that IC 3 and IC 4 display almost itentical $\hat{f}$.

4.2 Introduction of a Cleaning Factor into the numerical solution

4.2.1 Homogeneous Cleaning

Now, in order to estimate the efficacy of cleaning measures on CA population control and determine potential recommendations, we introduce a cleaning factor into our

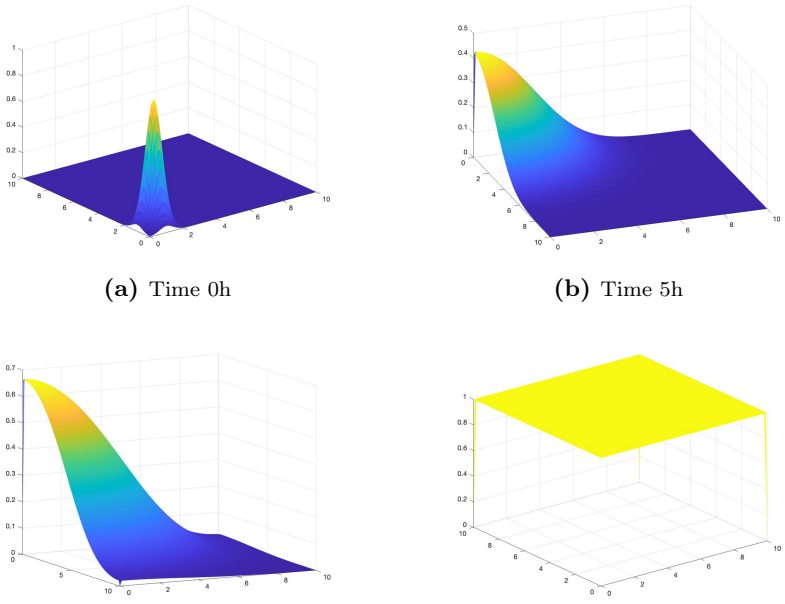

(a) Time 0h **(b)** Time 5h

(c) Time 10h **(d)** Time 48h

Figure 4.5: 3D plots of the FKPP numeric solutions with IC2

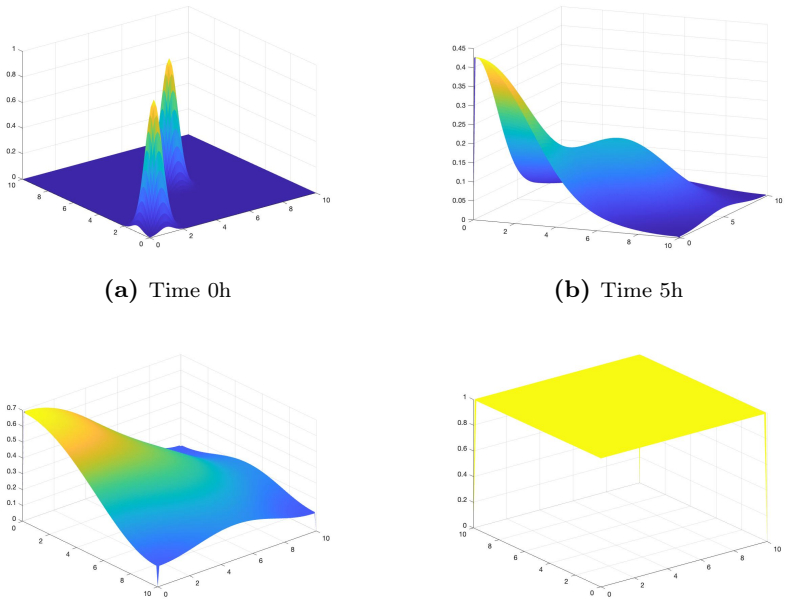

(a) Time 0h **(b)** Time 5h

(c) Time 10h **(d)** Time 48h

Figure 4.6: 3D plots of the FKPP numeric solutions with IC3

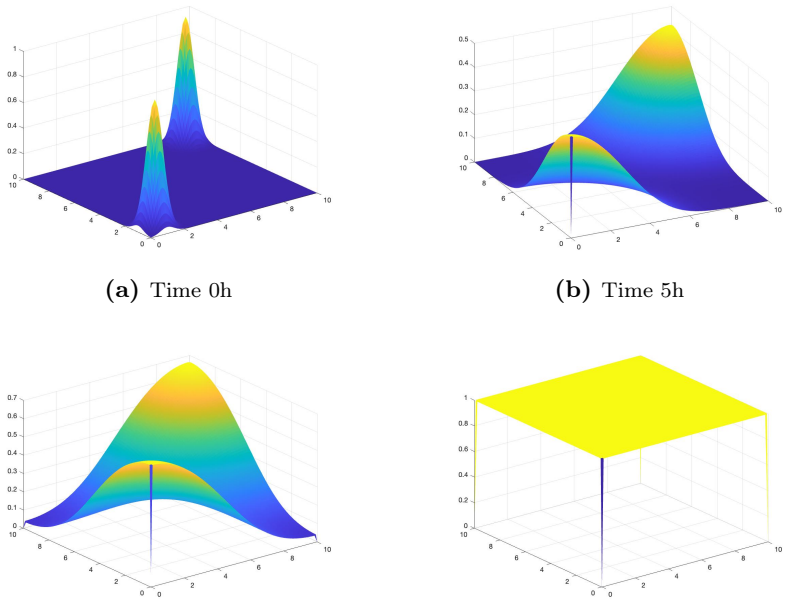

(a) Time 0h **(b)** Time 5h

(c) Time 10h **(d)** Time 48h

Figure 4.7: 3D plots of the FKPP numeric solutions with IC4

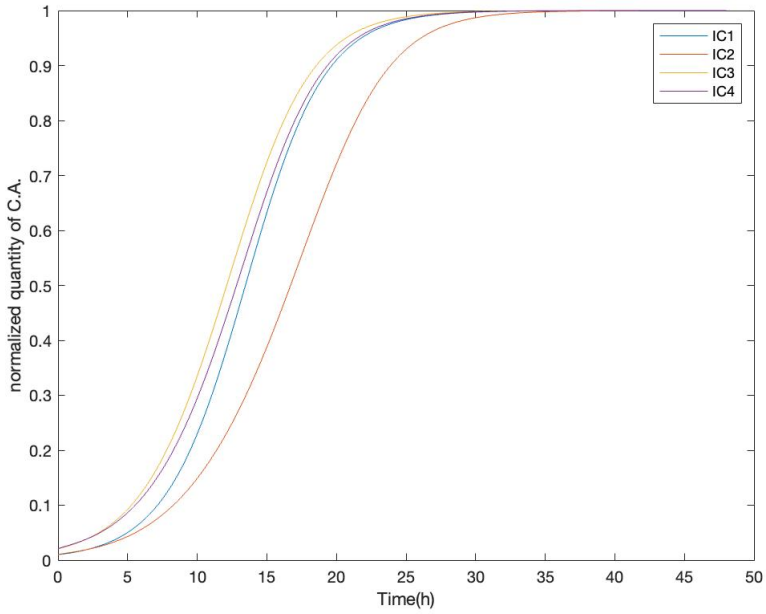

Figure 4.8: $\hat{f}$ estimated with different initial conditions

model. This cleaning factor is as described in Section 2.2. We periodically reduce the population of CA present in the ICU by a percentage in a homogeneous way.

We compare the values of

$$M = \frac{max_{i=1,\dots,n}[\hat{f}(t_i)]}{1,0197 \times 10^2} \tag{4.1}$$

for different combination of time intervals between cleaning (TI) and cleaning efficacy (CE). This represents the maximum quantity of CA present in the ICU relative to the worse case scenario where the whole ICU is infected $(1,0197 \times 10^2)$.

We choose to vary TI from 2 hours to 10 hours with a one hour increase. Cleaning more often than every $2h$ seems unrealistic and expensive, whereas cleaning less than every $10h$ appears to be too low for a healthcare environment with gravely ill patients who are very susceptible to any sort of infection.

The CE is equivalent to p as defined in Section 2.2 and thus CE has to be strictly between 0 and 1. The highest CE value we choose is 0.966 in order to model the efficacy of vaporized hydrogen peroxide (H_2O_2) on CA [1]. From the current literature on the efficacy of cleaning agents commonly used in healthcare environments, H_2O_2 appeared to be the most effective against CA. The next eight variations of CE go from 0.9 to 0.5, in 0.1 decreases, meaning that the lowest cleaning agent we consider reduces the CA quantity by 50% each time the ICU is cleaned. A cleaning agent that kills less than 50% of CA would be unlikely to be used in an ICU since the personnel is well trained and follows guidelines issued after laboratory research.

We observe that given a combination of CE and TI the values of M (defined in equation (4.1)) are equivalent to $\hat{f}(t = 0) = 0.0103$, meaning that the amount of CA never surpasses the quantity of the initial outbreak. Figure 4.9 and Table 4.1

show us that this happens for all TI except 10 hours when the cleaning agent is H_2O_2, corresponding to CE of 0.966. This suggests that a homogeneous cleaning of the entire ICU with H_2O_2 vapor could be an effective population control tool. In this table we can also observe how keeping either CE or TI constant and varying the other affects the value of M, which reflects in to some degree the efficacy of cleaning measures on CA population control. For example, if we keep CE = 0.7 and vary TI, we can see that up to TI = 4, we do not surpass the initial amount of CA (0.0103). However, for TI of 4 and up, we surpass this value and start approaching the worst case scenario ($M = 1$). As expected, the highest M is obtained in our simulations when TI = $10h$ and CE = 0.5. In this case $M = 0.9689$, which is quite close to 1, or our worse case scenario (no cleaning measures are taken). Meaning that if cleaning is not done often enough and with an effective enough cleaning agent almost no population control of CA is achieved. Furthermore, some cleaning agents that are not particularly effective against CA are quite effective against other microorganisms that might be present in the ICU and could compete with CA for resources [1]. The partial reduction of CA accompanied with complete removal of some of the competing microorganisms could increase the rate at which CA diffuses throughout the ICU and increase the risk of contamination for the patients.

The Figure 4.10 shows us how $\hat{f}(t)$ changes for $t \in [0, 48]$ when TI is 4 hours. We observe that for the CE of 0.966 and 0.8, the normalized amount of CA never goes above the initial amount of 0.0103. But we can see that it takes longer for the amount of CA to decrease in the second case and after $48h$ it is further from 0. For the case where the CE is lowered to 0.7, we rapidly surpass the initial amount of CA, but it still is quite far from reaching the worst case scenario (when no cleaning is introduced).

Table 4.1: Values of M for different combinations of TI and CE

TI (hours)		**2**	**3**	**4**	**5**	**6**	**7**	**8**	**9**	**10**
CE (%)	**96.6**	0.0103	0.0103	0.0103	0.0103	0.0103	0.0103	0.0103	0.0103	0.0185
	90	0.0103	0.0103	0.0103	0.0103	0.0103	0.0265	0.1591	0.3573	0.4875
	80	0.0103	0.0103	0.0103	0.0362	0.2644	0.4727	0.7144	0.8023	0.8476
	70	0.0103	0.0103	0.0865	0.3949	0.6540	0.7570	0.8493	0.8951	0.9226
	60	0.0103	0.0702	0.4587	0.6695	0.7918	0.8557	0.9049	0.9341	0.9525
	50	0.0122	0.4161	0.6707	0.7901	0.8631	0.9062	0.9369	0.9564	0.9689

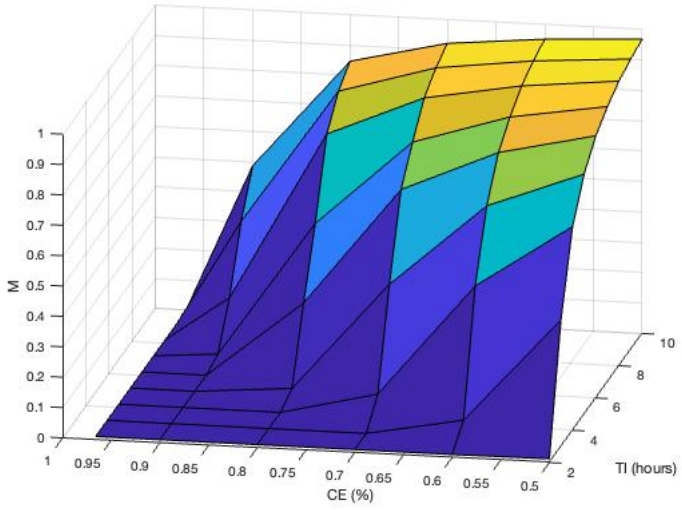

Figure 4.9: Surface plot of the maximum normalized quantity of CA given different CE and TI.

Overall, Table 4.1 shows us that in order to control CA population and keep its amount always under the initial amount present in the outbreak, cleaning of the ICU should be performed at most every $3h$. If cleaning is performed every $3h$ the cleaning efficacy of the agent should be at least 70%. If it is affordable to perform cleaning every $2h$, then the cleaning agent should have an efficacy of at least 60%. For cleaning efficacies of 50% and under, we do not achieve the desired population control.

4.2.2 Randomly distributed cleaning

The previous modeling of cleaning does not capture reality quite well. It is very hard to clean homogeneously everywhere, there will always be surfaces where less product of pressure is applied. There are some surfaces that are hard to reach, such as the inside of a tube, as well as surfaces, such as screens, that cannot be cleaned with some cleaning agents. Therefore, we propose a randomly distributed cleaning, where every point of the ICU has been cleaned by a certain amount, and this amount follows a probability density function. To define our randomly distributed cleaning

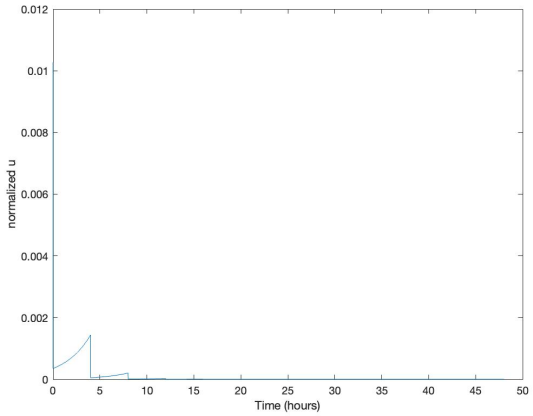

(a) CE = 0.966

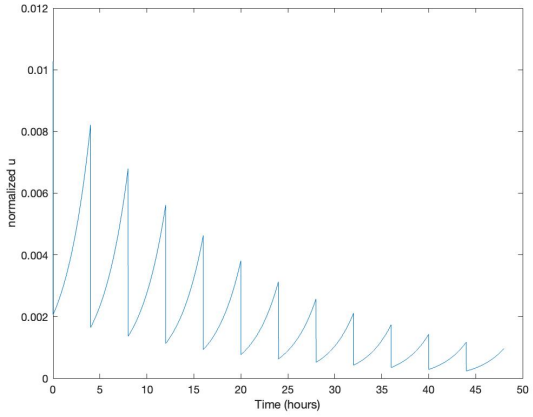

(b) CE = 0.8

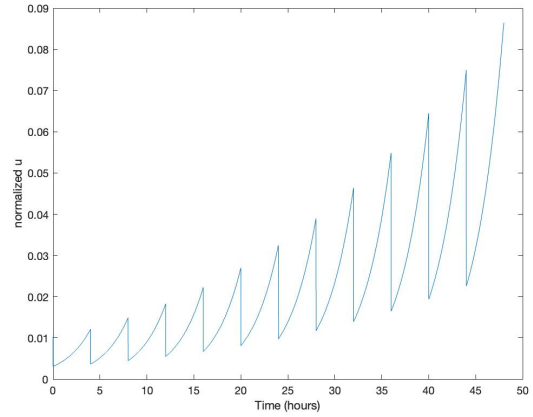

(c) CE = 0.7

Figure 4.10: Comparison of CE when TI is 4 hours.

factor, we will use the notions of probability space, random variable and its expected value and variance. For further details about probability and measure theory consult [3].

We suppose that that X, which represents the amount of CA killed by the cleaning agent (equivalent to CE previously defined) at a point (x, y) on the ICU plane is a random variable. Further, we assume that $E(X) = 0.8$, which means that the expected amount of C.A killed is 0.8 (we recall that the amount of CA is restricted to the interval $[0, 1]$). If we have n points where cleaning is performed, we suppose that the amounts of CA killed, $X_i, i = 1, \ldots, n$ are independent and identically distributed.

Because X must lie in $[0, 1]$, we decide to choose a probability with a support restricted to this interval. We propose a Beta distribution and will calculate its parameters so that its mean is 0.8. This probability distribution is left-skewed, meaning that most of its weight is located at the right side of $[0, 1]$, so that it is more likely that an amount of CA closer to 1 is killed.

Let X be a random variable in a probability space $(\Omega, \mathcal{F}, P)$. We say that X follows a Beta distribution with parameters α, β (denoted as $X \sim \text{Beta}(\alpha, \beta)$) if it has an associated measure μ such that for any $A \in \mathcal{B}$ (subset of the Borel σ-algebra of $\mathbb{R}$), we have

$$\mu(A) = \frac{1}{B(\alpha, \beta)} \int_A x^{\alpha-1}(1-x)^{\beta-1} I_{(0,1)}(x) m(dx), \tag{4.2}$$

Further the probability density function of X is

$$f(x, \alpha, \beta) = \frac{1}{B(\alpha, \beta)} x^{\alpha-1}(1-x)^{\beta-1} \tag{4.3}$$

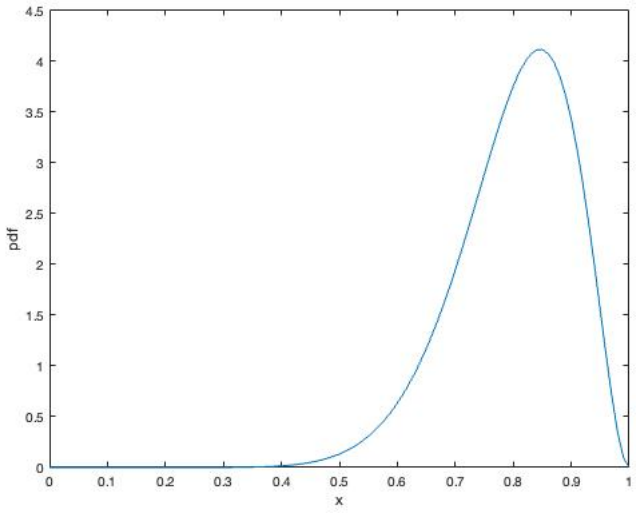

Figure 4.11: Probability density function of $Beta(12, 3)$

for any $x \in [0, 1]$ where $B(\alpha, \beta) = \frac{\Gamma(\alpha)\Gamma(\beta)}{\Gamma(\alpha+\beta)}$, $I_{(0,1)}$ denotes the characteristic function on $(0, 1)$, and $\alpha, \beta \in (0, \infty)$.

Then it is known that $E(X) = \frac{\alpha}{\alpha+\beta}$ and $Var(X) = \frac{\alpha\beta}{(\alpha+\beta)^2(\alpha+\beta+1)}$ [3].

As discussed before we set the expected value (mean) to be $E(X) = 0.8$. We also set the variance to be 0.01, $Var(X) = 0.01$, so that most of the amount of CA killed is in $[0.7, 0.9]$ since the standard deviation is 0.1. After solving the system we obtain α and β that give us the wanted behavior, we get $\alpha = 12, \beta = 3$, giving us

$$X \sim \text{Beta}(12, 3)$$

. The probability density function given by equation (4.3) with $\alpha = 12, \beta = 3$ is represented in Figure 4.11. We can see that as wanted, most of the weight is in $[0.7, 0.9]$.

For our simulations, the amount of CA at each point of the ICU plane is reduced by $1 - x,\ x \in (0, 1)$ where $X \sim \text{Beta}(12, 3)$. We then proceed to simulate cleaning

for TI of $2, 4, 8$ hours. Figure 4.12 shows us how the amount of CA changes through time as TI is changed. We can compare subplots (b) of figures 4.10 and 4.12, where the first one is simulated with a fixed CE of 0.8 and the second is simulated with expected CE of 0.8. We can see that the results are quite similar, both in shape and range of values. In both cases $M = 0.0103$, meaning that we never surpass the initial amount of CA.

However, here, we are assuming that there is no correlation between our n points where cleaning is performed which is not realistic. This can be clearly seen in Figure 4.14, where at 10h, where cleaning is performed, the surface displays many spikes as at each point the amount of CA killed, or CE, is independent, even for adjacent points. The other three subplots show us that the solution smoothes out after cleaning is performed. It is natural to assume that points nearby will have a similar amounts of CA killed. Hence, a generalization of the Beta distribution to the multivariate case (where each marginal distribution is a Beta distribution) with a correlation structure, such as the Dirichlet distribution would be more appropriate. We could also use a multivariate Normal distribution for our n points and then truncate it to $[0, 1]^n$.

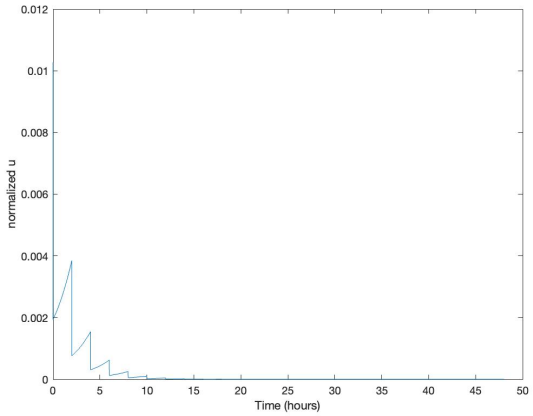

(a) TI $= 2h$

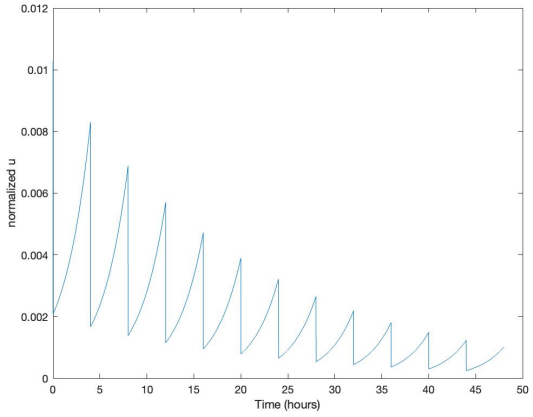

(b) TI $= 4h$

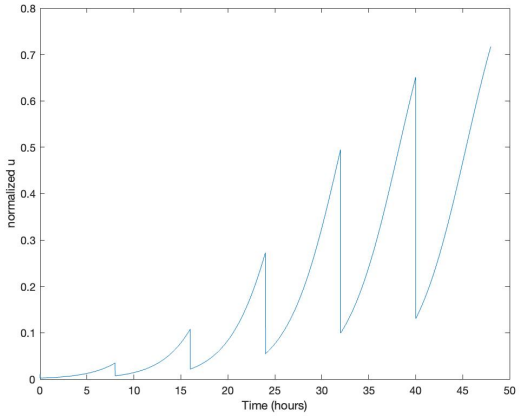

(c) TI $= 8h$

Figure 4.12: Comparison of TI when the amount of CA killed follows a Beta$(12, 3)$ distribution.

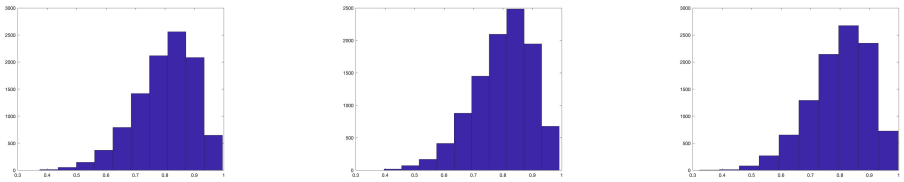

(a) TI = $2h$ **(b)** TI = $4h$ **(c)** TI = $8h$

Figure 4.13: Histograms of the amount of CA killed for the respective TI.

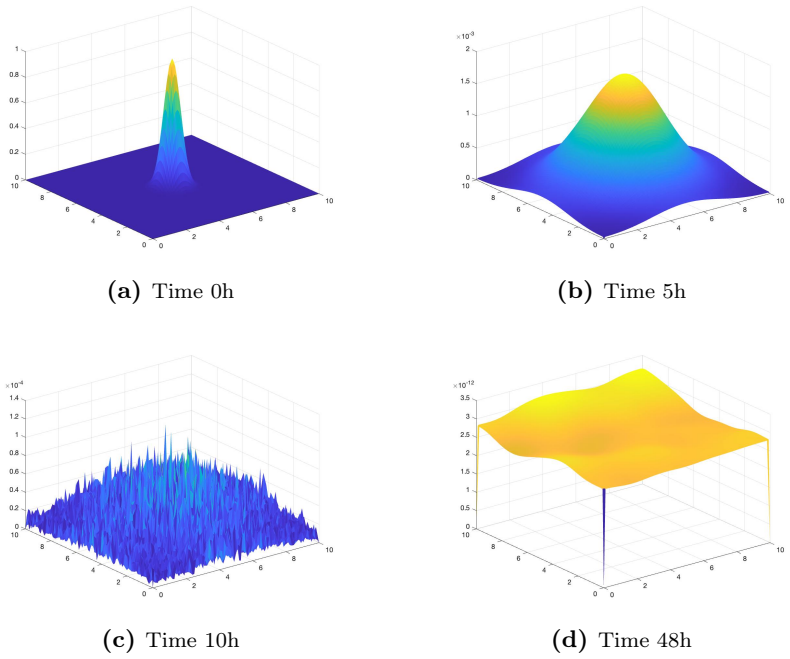

(a) Time 0h **(b)** Time 5h

(c) Time 10h **(d)** Time 48h

Figure 4.14: 3D plots of the FKPP numeric solutions with TI = 2 and CE following a Beta distribution

Discussion and Conclusion

We have built a FKPP reaction-diffusion model, which we solved numerically and then calibrated to real-life data of CA growth. After the calibration we have found that the speed at which the ICU gets completely infected depends, to a certain degree, on the location and number of outbreaks. In our simulations, we also showed that if cleaning is done often enough, and at a high enough frequency, the maximum amount of CA present in the ICU does not surpass the initial amount of the outbreak. If cleaning is performed every 3 hours the cleaning efficacy of the agent should be at least 70%. If cleaning is performed every 2 hours, then the cleaning agent should have an efficacy of at least 60%. Our results using fixed and random cleaning efficacy were very similar.

There are, however, great limitations in our model and the introduction of the cleaning factor that need to be addressed.

First, our model is calibrated with in-vitro growth of CA which is not equivalent to microbial growth in a health care environment. The ICU is kept at a temperature of 23^oC, whereas the strains in the observed data were incubated at 37^oC, which is a lot closer to the optimal temperature for CA growth. Therefore, we can expect CA

growth to be slower in an ICU, approaching a full contamination level at around 48 hours, as mentioned by ICU personnel, rather than 25 hours.

Secondly, our model does not account for the ecological pressures present in the microbial environment such as local extinction and colonization processes as different species compete for resources [13]. It is important to think about how cleaning can affect the environmental competition. Cleaning could perhaps reduce in a more significant way a microorganism that is highly competitive with CA, which would then allow CA access to more resources and accelerate its growth. Some cleaning agents such as H_2O_2 vapor have been shown to be more effective at killing non CA species [1].

Homogeneous cleaning is also an unreasonable assumption. Some of the ICU material cannot be cleaned as in depth as a simple plastic surface. Keyboards, screens, tubes, etc. cannot be always cleaned with all cleaning agents and in a in depth manner. Our simulations with randomly distributed cleaning efficacy appears to be a bit more realistic, although it lacks a covariance structure to model the fact that points nearby are more likely to be cleaned in a similar manner and provided with a very irregular cleaning pattern.

This model, however, indicates that the efficacy of the cleaning agent and how often the ICU room is cleaned greatly affects how well the yeast can be controlled.

Appendix

Mean Squared Error

The mean squared error is:

$$E \coloneqq \frac{1}{n}\sum_{i=1}^{n}\Big(f(t_i) - z_i\Big)^2 \tag{4.4}$$

where $\{t_1, t_2, \ldots, t_n\}$ is the set of times where CA's $A600nm$ (absorbance at $600nm$ wavelength) was measured and $\{z_1, z_2, \ldots, z_n\}$ is the set of measurements themselves. Minimizing E will give us that $u(x, y, t) > 0$ for all $0 \leq x \leq 10$, $0 \leq y \leq 10$, $25 \leq t \leq 48$.

Computationally, since we have built a mesh-grid to represent the plane of the ICU, we estimate for any $i \in \{1, 2, \ldots n\}$,

$$f(t_i) = \int_0^{10}\int_0^{10} u(x, y, t_i)dxdy$$

with

$$\hat{f}(t_i) = 0.1^2 \sum_{x,y \in \{0,0.1,0.2,\ldots,10\}} \sum u(x, y, t_i).$$

We can then define an estimate of the error E defined in (4.4) as:

$$\hat{E} \coloneqq \frac{1}{n} \sum_{i=1}^{n} \left(\hat{f}(t_i) - z_i \right)^2. \tag{4.5}$$

$\hat{E}$ is the target function to minimize we give the PSO algorithm in order to calibrate r and D simultaneously. When calculating $\hat{E}$, we normalize both $f(t_i)$ and z_i for $i = 1, \ldots, n$ by dividing them by their respective maximum so they both are restricted to the interval $[0, 1]$.

We search for (D, r) in $[0.0001, 1]^2$ and run the *particleswarm* function with a swarm size of 30 for 200 iterations and get $\hat{D} = 0.9803, \hat{r} = 0.3423$, and $\hat{E} = 0.0034$. We remark that 200 iterations were not needed as the algorithm stopped after 48 iteration because the relative change in the objective value was less than $1e{-}6$.

As we can see in Figure 4.16, the estimated curve follows more closely the larger observed values. This is because the mean squared error has bias towards values larger in magnitude. It is then appropriate to calibrate the model using a different type of error that takes into account the relative magnitude of the points and compare the results as was done in Chapter 4.

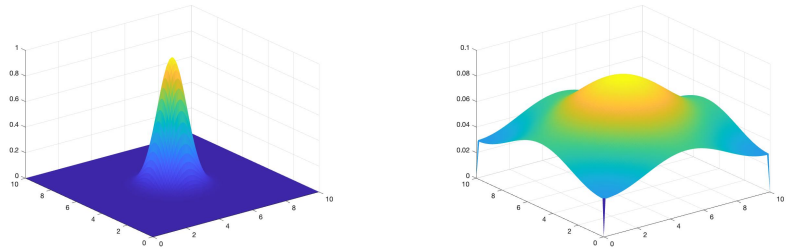

(a) Time 0h **(b)** Time 5h

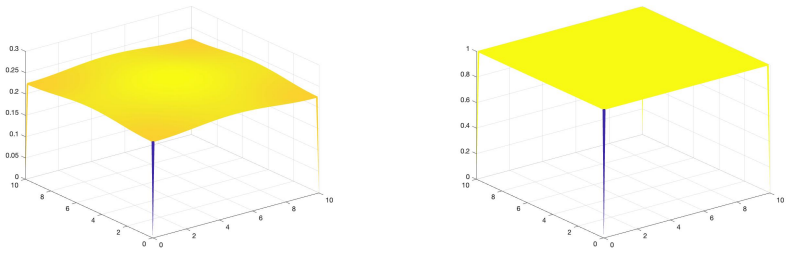

(c) Time 10h **(d)** Time 48h

Figure 4.15: 3D plots of the FKPP numeric solutions when $\hat{D} = 0.9803, \hat{r} = 0.3423$

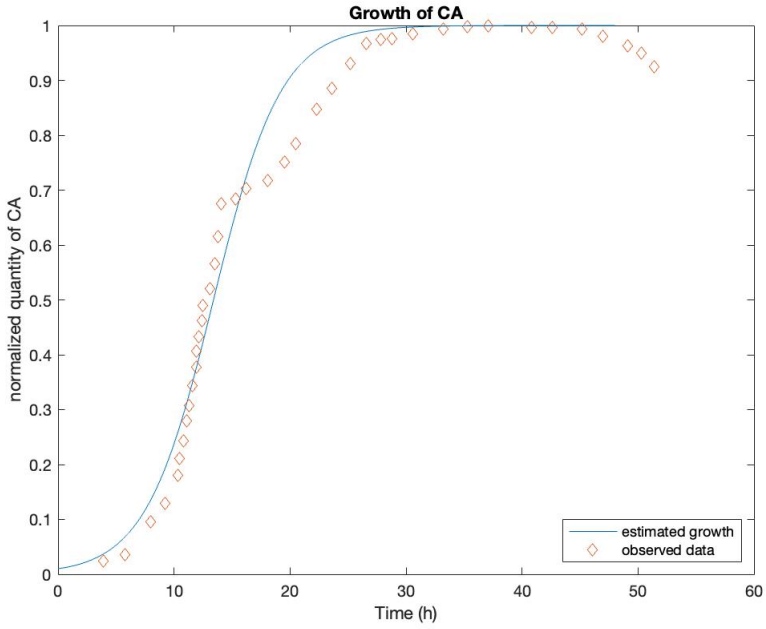

Figure 4.16: Observed *in vitro* growth of CA (points in orange) and $\hat{f}(t_i)$) (blue line) estimated using PSO.

Bibliography

[1] Alireza Abdolrasouli et al. "In vitro efficacy of disinfectants utilised for skin decolonisation and environmental decontamination during a hospital outbreak withiCandida auris/i". In: *Mycoses* 60.11 (2017), pp. 758–763. DOI: 10.1111/myc.12699 (cit. on pp. 28, 29, 40).

[2] *Antimicrobial resistance*. URL: https://www.who.int/news-room/fact-sheets/detail/antimicrobial-resistance (visited on 07/11/2022) (cit. on p. 5).

[3] Krishna B Athreya and Soumendra N Lahiri. *Measure Theory and Probability Theory*. Springer New York, 2006. DOI: 10.1007/978-0-387-35434-7 (cit. on pp. 33, 34).

[4] Douglas M Bates and Saikat DebRoy. *Nonlinear least squares*. 2016. URL: https://stat.ethz.ch/R-manual/R-devel/library/stats/html/nls.html (visited on 07/11/2022) (cit. on p. 13).

[5] Douglas M. Bates and Donald G. Watts, eds. *Nonlinear Regression Analysis and Its Applications*. John Wiley & Sons, Inc., 1988. DOI: 10.1002/9780470316757 (cit. on pp. 11, 13).

[6] Nancy A Chow et al. "Multiple introductions and subsequent transmission of multidrug-resistant Candida auris in the USA: a molecular epidemiological survey". In: *The Lancet Infectious Diseases* 18.12 (2018), pp. 1377–1384. DOI: 10.1016/s1473-3099(18)30597-8 (cit. on p. 3).

[7] Anuradha Chowdhary, Cheshta Sharma, and Jacques F. Meis. "Candida auris: A rapidly emerging cause of hospital-acquired multidrug-resistant fungal infections globally". In: *PLOS Pathogens* 13.5 (2017). Ed. by Deborah A. Hogan, e1006290. DOI: 10.1371/journal.ppat.1006290 (cit. on p. 3).

[8] Andrea Cortegiani et al. "Epidemiology, clinical characteristics, resistance, and treatment of infections by Candida auris". In: *Journal of Intensive Care* 6.1 (2018). DOI: 10.1186/s40560-018-0342-4 (cit. on p. 4).

[9] Lawrence Evans. *Partial Differential Equations*. American Mathematical Society, 2010. DOI: 10.1090/gsm/019 (cit. on p. 9).

[10] David W. Eyre et al. "A iCandida auris/i Outbreak and Its Control in an Intensive Care Setting". In: *New England Journal of Medicine* 379.14 (2018), pp. 1322–1331. DOI: 10.1056/nejmoa1714373 (cit. on p. 4).

[11] Leiwen Fu et al. "Study on growth characteristics of Candida auris under different conditions in vitro and its in vivo toxicity". In: *Zhejiang da xue xue bao, Journal of Zhejiang University. Medical Sciences* 40.7 (2020), pp. 1049–1055 (cit. on p. 13).

[12] J. Kennedy and R. Eberhart. "Particle swarm optimization". In: *Proceedings of ICNN'95 - International Conference on Neural Networks*. IEEE. DOI: 10.1109/icnn.1995.488968 (cit. on p. 18).

[13] Juan E. Keymer et al. "Bacterial metapopulations in nanofabricated landscapes". In: *Proceedings of the National Academy of Sciences* 103.46 (2006), pp. 17290–17295. DOI: 10.1073/pnas.0607971103 (cit. on p. 40).

[14] Emily Larkin et al. "The Emerging Pathogen Candida auris: Growth Phenotype, Virulence Factors, Activity of Antifungals, and Effect of SCY-078, a Novel Glucan Synthesis Inhibitor, on Growth Morphology and Biofilm Formation". In: *Antimicrobial Agents and Chemotherapy* 61.5 (2017). DOI: 10.1128/aac.02396-16 (cit. on p. 4).

[15] Patrick Lascaux. *Lectures on Numerical Methods for Time Dependent Equations: Applications to Fluid Flow Problems*. Vol. 52. Tata Institute of Fundamental Research, 1976 (cit. on p. 16).

[16] Jordan Lee and Mr Sungwoo Jeong. *Stability of Finite Difference Schemes on the Diffusion Equation with Discontinuous Coefficients*. 2017 (cit. on p. 16).

[17] Shabir A. Lone and Aijaz Ahmad. "Candida auris —the growing menace to global health". In: *Mycoses* 62.8 (2019), pp. 620–637. DOI: 10.1111/myc.12904 (cit. on p. 5).

[18] Franklin D. Lowy. "Antimicrobial resistance: the example of Staphylococcus aureus". In: *Journal of Clinical Investigation* 111.9 (2003), pp. 1265–1273. DOI: 10.1172/jci18535 (cit. on p. 5).

[19] Amauri J. Paula, Geelsu Hwang, and Hyun Koo. "Dynamics of bacterial population growth in biofilms resemble spatial and structural aspects of urbanization". In: *Nature Communications* 11.1 (2020). DOI: 10.1038/s41467-020-15165-4 (cit. on pp. 6, 16).

[20] *Principles of Epidemiology*. 2012. URL: https://www.cdc.gov/csels/dsepd/ss1978/lesson3/section3.html (visited on 07/11/2022) (cit. on p. 5).

[21] Nira Rabin et al. "Biofilm formation mechanisms and targets for developing antibiofilm agents". In: *Future Medicinal Chemistry* 7.4 (2015), pp. 493–512. DOI: 10.4155/fmc.15.6 (cit. on p. 4).

[22] Johanna Rhodes and Matthew C Fisher. "Global epidemiology of emerging Candida auris". In: *Current Opinion in Microbiology* 52 (2019), pp. 84–89. DOI: 10.1016/j.mib.2019.05.008 (cit. on pp. 4, 5).

[23] Kazuo Satoh et al. "Candida auris sp. nov., a novel ascomycetous yeast isolated from the external ear canal of an inpatient in a Japanese hospital". In: *Microbiology and Immunology* 53.1 (2009), pp. 41–44. DOI: 10.1111/j.1348-0421.2008.00083.x (cit. on p. 3).

[24] U.K. Shyni and R. Lavanya. "A study on transmission dynamics of the emerging Candida Auris infections in Intensive Care Units: Optimal control analysis and numerical computations". In: *Physica A: Statistical Mechanics and its Applications* 561 (2021), p. 125253. DOI: 10.1016/j.physa.2020.125253 (cit. on p. 4).

[25] Vladimir M Tikhomirov. *Selected Works of AN Kolmogorov: Volume I: Mathematics and Mechanics*. Vol. 25. Springer Science & Business Media, 1991, pp. 242–245 (cit. on pp. 6–8).

[26] Rory M. Welsh et al. "Survival, Persistence, and Isolation of the Emerging Multidrug-Resistant Pathogenic Yeast Candida auris on a Plastic Health Care Surface". In: *Journal of Clinical Microbiology* 55.10 (2017). Ed. by Daniel J. Diekema, pp. 2996–3005. DOI: 10.1128/jcm.00921-17 (cit. on p. 5).

[27] R. Wise. "Antimicrobial resistance: priorities for action". In: *Journal of Antimicrobial Chemotherapy* 49.4 (2002), pp. 585–586. DOI: 10.1093/jac/49.4.585 (cit. on p. 5).